Manuscript refereed by Dr Gian Pietro De Gaudenzi (F.I.L.M.S. - Gruppo OMCD, Italy)

Influence of NbC and TaNbC Additions on WC-Ni based Nanostructured Hardmetals

Tamara Aleksandrov Fabijanić[1] tamara.aleksandrov@fsb.hr; Johannes Pötschke[2] johannes.poetschke@ikts.fraunhofer.de; ; Markus Mayer[2] markus.mayer@ikts.fraunhofer.de; Mateja Šnajdar Musa[3] mateja.snajdar@uniri.hr

[1]University of Zagreb, Faculty of Mechanical Engineering and Naval Architecture, Department of Materials, Laboratory for Testing Mechanical Properties, Ivana Lucica 5, 10000 Zagreb, Croatia
[2]Fraunhofer IKTS, Winterbergstrasse 28, 01277 Dresden, Germany
[3]Department of Polytechnics, University of Rijeka, Sveucilisna avenija 4, 51000 Rijeka, Croatia

Abstract

The need for Co replacement with alternative binders is imperative in hardmetals research due to environmental and health issues, high cost, and inferior corrosion properties. In combination with nano WC powders, alternative binders could reach the properties of WC-Co hardmetals with improved corrosion resistance. Nickel as a binder is one of the best cobalt alternatives due to its similar properties and enhanced electrochemical corrosion resistance. Previous studies indicated that adding niobium carbide to WC-Co hardmetals significantly refines grain size and limits grain growth. Depending on the amount of NbC in hardmetals, transverse rupture strength, hardness, and wear resistance can be improved. In contrast, TaNbC significantly improves oxidation, thermal and wear resistance, and hot-hardness. In this work, microstructural characteristics and mechanical properties were investigated by observing the influence of adding NbC and TaNbC to starting mixtures with a Ni content of 9 wt.% and a mean particle size of tungsten carbide of approximately 150 nm.

Introduction

Compositions of tungsten carbide (WC) and cobalt (Co) binder with different additions have been widely investigated and are commercially available. Alternative binder metals such as Nickel (Ni) and Iron (Fe) were later introduced to improve WC-based hardmetals corrosion resistance [1-3]. Studies of WC-Ni systems showed a better corrosion and oxidation resistance in comparison to Co binder based systems [3,4]. Most recent studies aim to utilize Ni binder for achieving better mechanical properties while reducing the high cost of raw material primarily associated with the high Co price and its negative environmental impact and health hazard issues [5-7]. However, early studies on WC-Ni hardmetals reported lower strength and hardness than Co binder systems [8,9]. Regardless of the binder material used, the addition of different types of cubic carbides such as Cr_3C_2, TaC, TiC, and VC has shown to be necessary to limit the grain growth during sintering in grades with WC grain sizes below 1 µm [10-12]. Information on the influence of different grain growth inhibitor (GGI) combinations on the grain growth inhibition process and resulting microstructural characteristics of consolidated hardmetals with binder materials other than Co is relatively scarce. Studies have shown that VC, TaC and Cr_3C_2 provide significant grain size refinement effects [13, 14]. Only a few published studies focused on NbC and TaNbC as grain growth inhibitors in nanostructured WC-Co hardmetals [15, 16]. Previous studies indicate that the addition of NbC to conventional WC-Co hardmetals significantly refines WC grain size and limits grain growth [17]. Besides grain refinement, NbC also improves mechanical properties such as transverse rupture strength, hardness, and wear resistance [18]. In literature, there is no published research on NbC and TaNbC influence on mechanical properties and microstructural characteristics of nanostructured hardmetals with alternative binders. Conventional WC-Co hardmetals are not the best solution for the petroleum and chemical industry, considering they exhibit low corrosion stability [19, 20]. Therefore, there is a need for new innovative materials with comparable mechanical properties to cobalt bonded nanostructured hardmetals. To achieve desired and similar mechanical properties, the solution to that problem could be using WC nanoparticles with NbC and TaNbC as multifunctional powder and $C_{r3}C_2$ as a grain growth inhibitor. This study investigates the effect of NbC and TaNbC added to WC-Ni hardmetals, focusing on microstructure development during sintering, grain refinement effectiveness, and mechanical properties.

Materials and Methods

Two types of starting mixtures with the same WC powder and Ni binder content of 9 wt.% were prepared. WC powder has an average grain size of d_{BET}<150 nm and a specific surface area (BET) of 2.9 m²/g. Used Ni powder has a fisher particle size of 2.6 µm. Since GGIs have been shown to

© European Powder Metallurgy Association (EPMA)

strongly contribute to grain size refinement effects, 1 wt. % Cr_3C_2 with a fisher particle size of 1.5 µm was added to both starting mixtures. Different types of cubic carbides were added to the starting mixtures: NbC with a fisher particle size of 0.9 µm was added to the first mixture, while TaNbC with the Ta:Nb ratio of 83.1/9.6% and a fisher particle size of 1.1 µm was used in the second. A horizontal ball mill was used for powder mixing/homogenization (24 h, powder ball ration of 1:10). An overview of starting powders and mixtures characteristics is given in Table 1.

Table 1: Starting powders and mixtures characteristics

Mixture	Starting powders	Content, wt. %
WC - 9Ni - NbC	WC DN 3.0 (H. C. Starck Tungsten)	rest
	AMPERSINT MAP Ni (Höganäs)	9
	Cr_3C_2 160 (Höganäs)	1
	NbC HGS (H.C. Starck)	0.5
WC - 9Ni - TaNbC	WC DN 3.0 (H. C. Starck Tungsten)	rest
	AMPERSINT MAP Ni (Höganäs)	9
	Cr_3C_2 160 (Höganäs)	1
	TaNbC HGS (H.C. Starck)	0.5

After milling and vacuum chamber drying, mixtures were sieved with a 315 µm sieve. Compacting of bending bar samples was conducted by uniaxial die pressing with a pressure of 200 MPa at room temperature on a hydraulic press. After debindering in H_2 containing atmosphere, both types of samples were directly sintered using a single-cycle sinter HIP process at a temperature of 1450 ºC and pressure of 60 bar for 45 min. Post-production sample characterization included density measurements by Archimedes principle using Metler Toledo range scale according to ISO 3369:2006. The porosity and possible unbound carbon presence were determined by comparing the polished surfaces with photo micrographs given in the ISO 4505:1978 standard. The occurrence of η-phase was checked by detailed analysis performed by optical microscopy (Olympus, Shinjuku City, Tokyo, Japan) after etching in Murakami reagent for 2 seconds. Microstructure analysis consisted of field emission scanning electron microscopy FESEM (Zeiss, Oberkochen, Germany), XRD analysis and EBSD analysis. Characterization of the mechanical properties included measurement of Vickers hardness and fracture toughness. The instrumented indentation test was conducted using Anton Paar micro combi tester MCT³ with Vickers indenter to determine the micro-mechanical properties of both types of samples. The force of 500 mN was applied, and a matrix of 24 indentations was made on each sample type. Poisson's ratio of 0.24 was assumed.

Results

Microstructural characteristics of consolidated samples

Table 2: Characteristics of consolidated samples with different types of added cubic carbides

Sample	Density g/cm³	Rel. Density, %	ISO Porosity			d_{WC}, nm
			A	B	C	
WC-9Ni-1Cr_3C_2-0.5NbC	14.45	100.2	A00-A02	B00	C00	267
WC-9Ni-1Cr_3C_2-0.5TaNbC	14.50	100.2	A00-A02	B00	C00	284

Consolidated samples achieved the theoretical density. The polished surfaces of both samples are mostly without porosity or uncombined carbon. In some places on the polished surface, some small pores are visible. Etching for 2 seconds in a Murakami reagent for η-phase evaluation revealed the presence of clusters on the surfaces of both samples, seen as star-like structures (Figure 1). These areas have similarity to η-phases (ISO 4499-4:2016). The star-like structures are more prominent on the WC-9Ni-1Cr_3C_2-0.5NbC sample (Figure 1a). The WC grain size d_{WC} measured by a conventional linear intercept method showed a slightly smaller grain size for the WC-9Ni-1Cr_3C_2-0.5NbC sample, later confirmed by FESEM analysis. Both samples have a mean WC grain size d_{WC}>200 nm and can be classified as near-nanostructured hardmetals. Microstructure FESEM analysis (see Figure 2.) confirmed a uniform distribution of WC grains without abnormal grain growth. However, within the WC-9Ni-1Cr_3C_2-0.5TaNbC sample, some larger WC grains were detected. The presence of structures/clusters distributed over the entire sample was confirmed for both samples. Since the density of the η-phase is higher than the Ni density, it would be of a lighter shade of grey on FESEM micrographs using a SE or ESB detector.

© European Powder Metallurgy Association (EPMA)

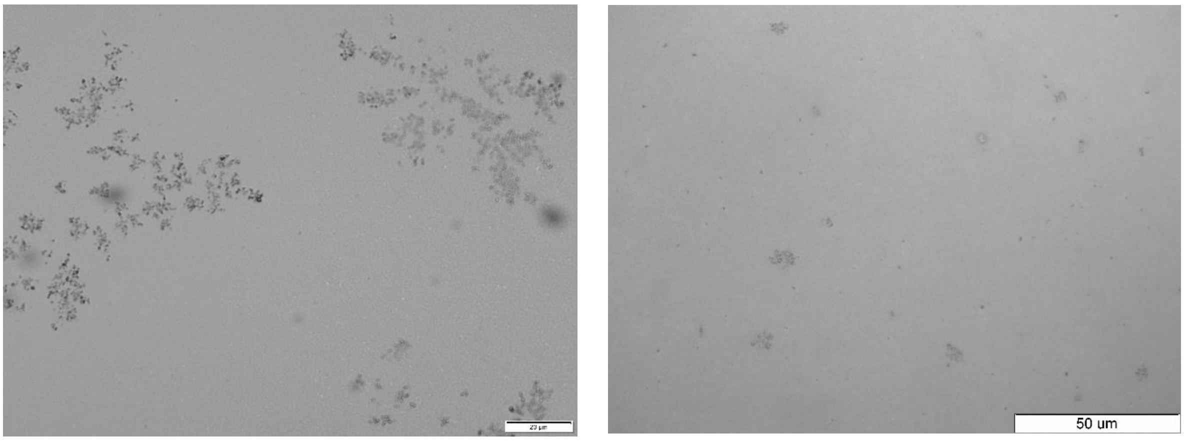

a) b)

Figure 1. Etched sample microstructure of sample a) WC-9Ni-1Cr_3C_2-0.5NbC b) WC-9Ni-1Cr_3C_2-0.5TaNbC

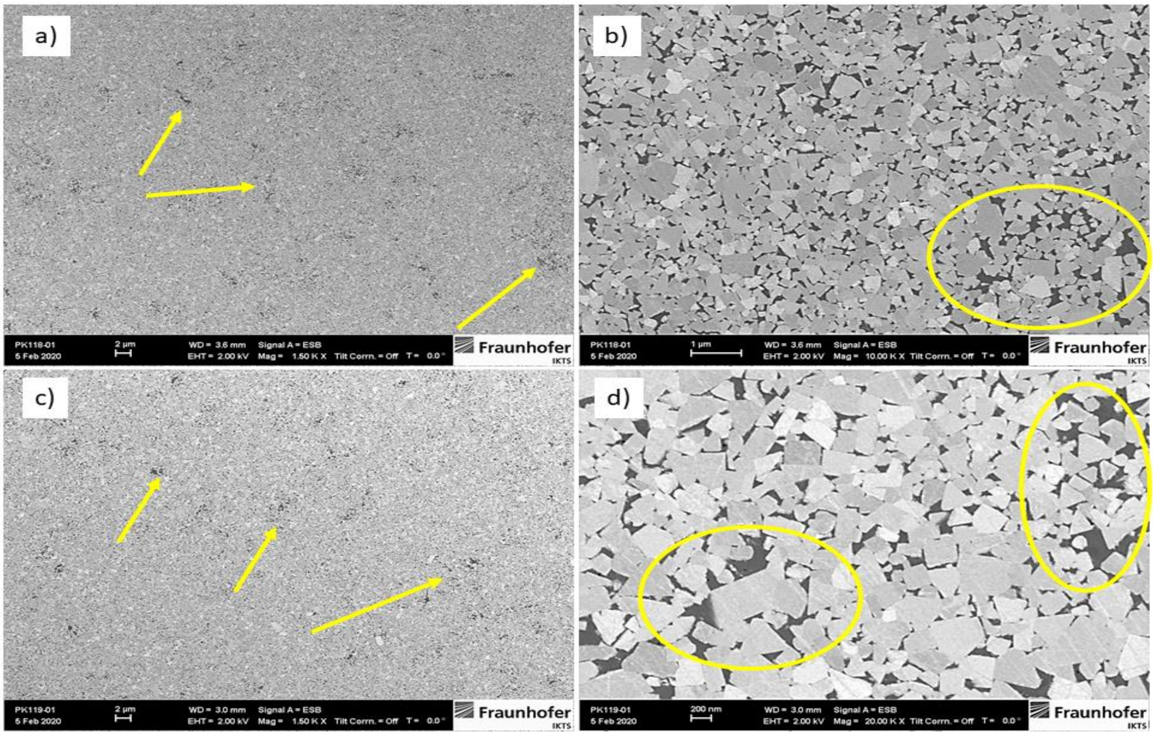

Figure 2. FESEM micrographs of the unetched samples where light grey particles are WC, medium grey particles are cubic carbides, and dark regions correspond to Ni binder. (a)(b) clusters detected on WC-9Ni-1Cr_3C_2-0.5NbC sample; (c) (d) clusters detected on WC-9Ni-1Cr_3C_2-0.5TaNbC sample

Since similar observed clusters were linked to the formation of complex Ni, Cr and Nb containing cubic carbide precipitations, [10,14] an EBSD mapping and EDS analysis of W, Ni, Nb and Cr was done to identify the WC, Ni, NbC and Cr_3C_2 phases within the microstructure. EDS results for both samples are shown in Fig. 3, and the EBSD results for the WC-9Ni-1Cr_3C_2-0.5NbC sample are shown in Figure 4.

© European Powder Metallurgy Association (EPMA)

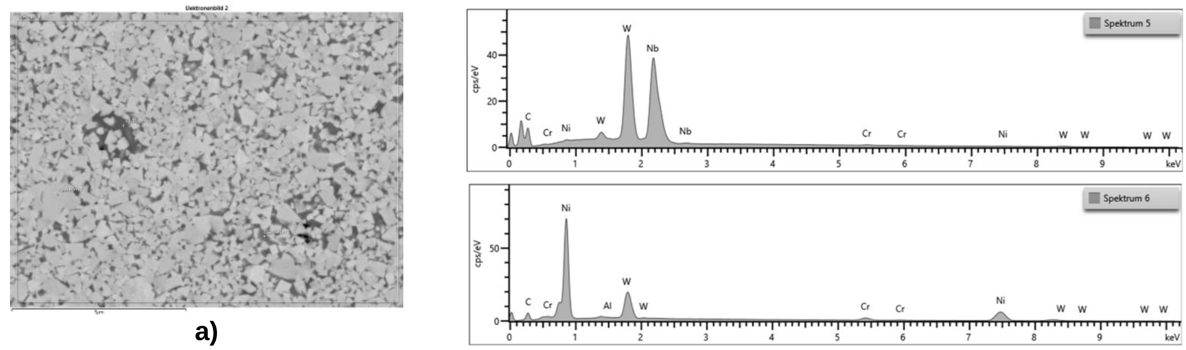

a)

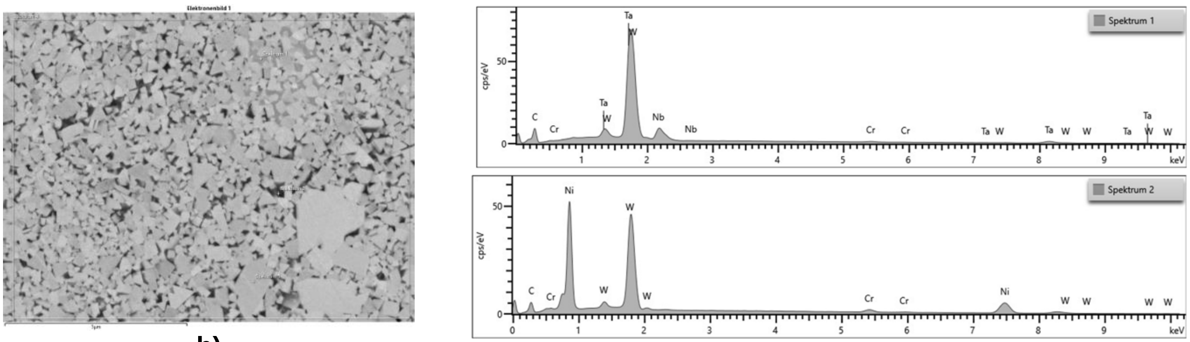

b)

Figure 3. EDS analysis a) WC-9Ni-1Cr_3C_2-0.5NbC b) WC-9Ni-1Cr_3C_2-0.5TaNbC

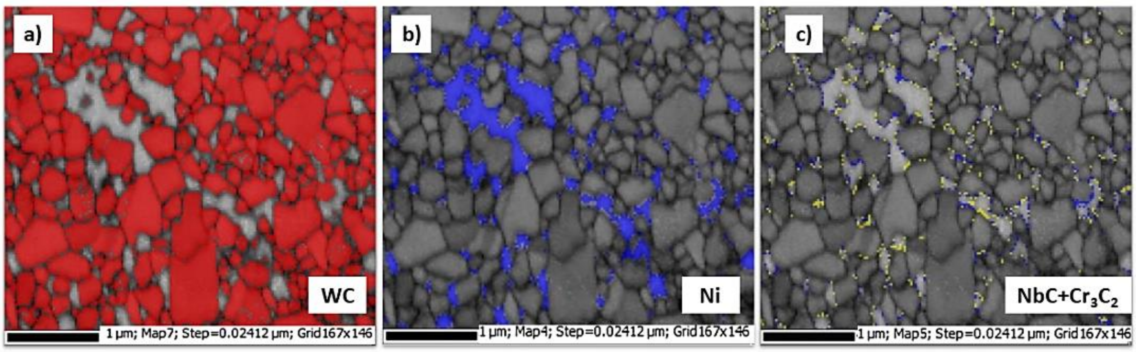

Figure 4. EBSD map of the same region of WC-9Ni-1Cr_3C_2-0.5NbC

WC and Ni phases were identified as the main phases, with NbC and Cr_3C_2 cubic carbides detected mostly at grain boundaries. Cubic carbide precipitation from the added cubic carbides was only identified by EDS (Figure 5) and EBSD analysis and light optical analysis.

Further investigations done by XRD indicated WC with hexagonal crystal structure and an alloyed Ni binder with cubic structure, as shown in Figure 5. The binder peak of both samples corresponds quite well to a Cr alloyed Ni_3Cr phase (PDF file 01-071-7595). No peaks for η- phase, like Ni_2W_4C, Ni_3W_3C or Ni_6W_6C were present in any samples. Comparing obtained patterns with those in other studies [21] of WC-Ni systems where η-phase peaks are identified at certain 2 theta values it is evident that no such peaks are seen for the here studied WC-9Ni-1Cr_3C_2-0.5NbC as well as the WC-9Ni-1Cr_3C_2-0.5TaNbC samples. This confirms the absence of η-phase and the presence of a heavily alloyed binder phase. However, also none of by EDS and EBSD identified carbide precipitations were detected by XRD. Possible reasons are either the too low amount of just around 1 wt.% or a complex less structured lattice of these precipitations.

© European Powder Metallurgy Association (EPMA)

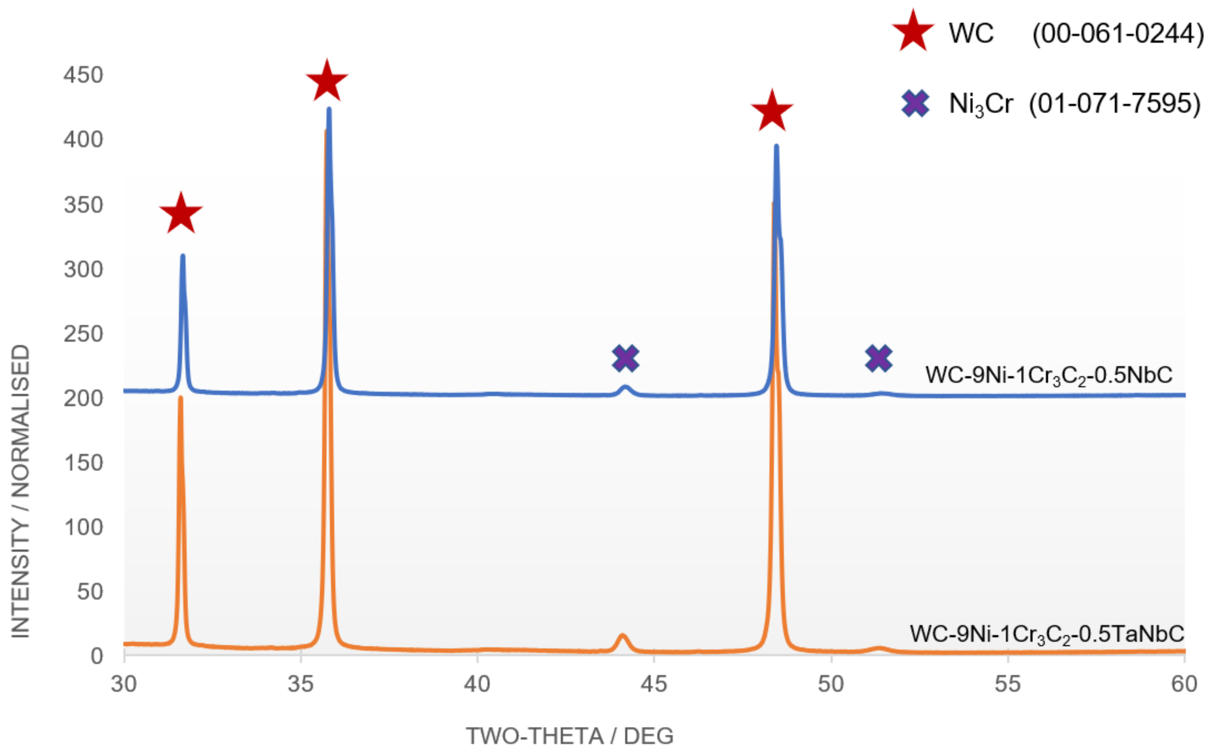

Figure 5. XRD pattern for samples $WC\text{-}9Ni\text{-}1Cr_3C_2\text{-}0.5NbC$ and $WC\text{-}9Ni\text{-}1Cr_3C_2\text{-}0.5TaNbC$

Mechanical testing results

The average hardness of 1810±10 HV10 was measured for the $WC\text{-}9Ni\text{-}1Cr_3C_2\text{-}0.5NbC$ sample and 1790±10 HV10 for the $WC\text{-}9Ni\text{-}1Cr_3C_2\text{-}0.5TaNbC$ sample using a standard HV10 tester. Fracture toughness of 8.2±0.2 MPa√m was obtained for the $WC\text{-}9Ni\text{-}1Cr_3C_2\text{-}0.5NbC$ sample and 8.2±0.1 MPa√m for the $WC\text{-}9Ni\text{-}1Cr_3C_2\text{-}0.5TaNbC$ sample. Instrumented indentation test IIT results include indentation plane strain modulus (E), indentation modulus (E_{IT}), indentation hardness (H_{IT}), Vickers instrumented hardness (HV_{IT}), stiffness (S), elastic work (W_{elast}), plastic work (W_{plast}), indentation work ratio (η_{IT}), and indentation creep (C_{IT}), and are presented in Table 3.

Table 3: Instrumented indentation test results

				$WC\text{-}9Ni\text{-}1Cr_3C_2\text{-}0.5NbC$					
	E, GPa	**E_{IT}, GPa**	**H_{IT}, MPa**	**HV_{IT} (HV)**	**S, mN/nm**	**W_{elast}, pJ**	**W_{plast}, pJ**	**η_{IT}, %**	**C_{IT}, %**
Min	562	530	19234	1815	2.078	66515	118702	33.6	1.28
Max	678	639	22610	2134	2.416	70458	131924	36.8	2.23
Mean	**622**	**586**	**20815**	**1965**	**2.257**	**68459**	**127459**	**35.0**	**1.76**
St dev	36.8	34.6	842.7	79.54	0.093	1046	3155.8	0.01	0.21
				$WC\text{-}9Ni\text{-}1Cr_3C_2\text{-}0.5TaNbC$					
	E, GPa	**E_{IT}, GPa**	**H_{IT}, MPa**	**HV_{IT} (HV)**	**S, mN/nm**	**W_{elast}, pJ**	**W_{plast}, pJ**	**η_{IT}, %**	**C_{IT}, %**
Min	613	578	17894	1689	2.219	55876	128196	28.5	1.53
Max	949	894	21453	2025	3.018	66880	142497	34.0	2.36
Mean	**706**	**665**	**19889**	**1877**	**2.497**	**62619**	**134869**	**32.0**	**1.94**
St dev	86.3	81.4	922.9	87.10	0.209	3243.1	4414.6	0.02	0.24

Higher hardness values H_{IT} were measured by IIT compared to Vickers hardness HV10 measurement for both samples related to the indentation size effect ISE. ISE represents the increase in hardness

© European Powder Metallurgy Association (EPMA)

with decreasing penetration depth, especially at depths of less than a few micrometres, and is connected to dislocation microstructures and how they vary with indentation size [23]. Regardless of the test method used, higher hardness values were measured for the WC-9Ni-1Cr_3C_2-0.5NbC sample indicating that the addition of pure NbC in comparison to TaNbC results in a higher overall hardness. Higher W_{elast} and η_{IT} were also obtained for the WC-9Ni-1Cr_3C_2-0.5NbC sample, indicating here too that internal resistance to deformation under applied load is higher in case of NbC addition. C_{IT} represents the relative change in the indentation depth during the application of constant force over 30 seconds and is lower for the WC-9Ni-1Cr_3C_2-0.5NbC sample indicating higher resistance to time-dependent deformation under the constant stress at room temperature.
On the other hand, higher values of W_{plast}, S, *E and* E_{IT} were measured for the WC-9Ni-1Cr_3C_2-0.5TaNbC sample indicating that TaNbC added to the starting WC-Ni hardmetal mixture contributes to higher stiffness of the material. Here, the stiffness of the contact S includes a contribution from both the sample and the test device itself, but it still represents the resistance of the material to being deformed elastically and corresponds to higher values of W_{plast}, *E and* E_{IT}.

Conclusions

The following conclusions can be drawn from the conducted research:

- Fully dense WC-Ni hardmetals with the addition of Cr_3C_2, NbC and TaNbC were developed using one cycle sinter-HIP process. Both samples achieved a homogeneous microstructure with relatively uniform WC grain-size distribution, without abnormal grain growth but a slightly inhomogeneous Ni binder distribution.
- Etching with Murakami for 2 sec. shows an additional third phase with star-like structures in the light optical microscopy. Further investigations showed, that these structures are not η-phase but precipitation of the used carbide additions. The results show, that for Ni bonded hardmetals already etching for 2 sec. is enough for revealing cubic carbide precipitations, in contrast to Co bonded hardmetals where such carbide precipitations are only expected after > 5 sec. [22].
- The use of Cr_3C_2 and Nb/TaNbC addition with in total 1.5 wt.% in the starting mixtures of WC-9 Ni is thus to high for a full solution within the binder phase and leads to the formation/precipitation of cubic lattice.
- The Ni binder is highly alloyed with Cr, resulting in a XRD peak shift to a peak position constating with a cubic $CrNi_3$ phase
- Achieved mechanical properties are comparable to mechanical properties of Co-bonded nanostructured hardmetals. Higher H_{IT}, W_{elast} *and* η_{IT} values were obtained for WC-9Ni-1Cr_3C_2-0.5NbC sample, while higher *E*, E_{IT}, *S*, W_{plast} and C_{IT}, were obtained for WC-9Ni-1Cr_3C_2-0.5TaNbC sample.

Acknowledgements

This work is supported in part by the Croatian Science Foundation under Project Number UIP-2017-05-6538 Nanostructured hardmetals – New challenges for Powder Metallurgy. This work is supported by European Regional Development Fund under the Project number KK.01.2.1.01.0079 Research and development of nanostructured hardmetals for the development of new products NANO-PRO.

References

[1] Sun, J.; Zhao, J.; Gong, F.; Ni, X.; Li, Z. (2019). Development and Application of WC-Based Alloys Bonded with Alternative Binder Phase, Critical Reviews in Solid State and Materials Science. *44,* 211-238.
[2] Jayaraj, J.; Olsson, M. (2021). Effect of tribo-layer on the corrosion behavior of WC-Co and WC-Ni cemented carbides in synthetic mine water, Int J Refract Hard Met., *100*, 105621.
[3] Steinlechner, R.; de Oro Calderon, R.; Koch,T.; Linhardt, P.; Schubert, W.A. (2022). A study on WC-Ni cemented carbides: Constitution, alloy compositions and properties, including corrosion behaviour, , Int J Refract Hard Met., *103*, 105750.
[4] Ghasali, E.; Ebadzadeh, T.; Alizadeh, M.; Razavi, M. (2018). Mechanical and microstructural properties of WC-based cermets: a comparative study on the effect of Ni and Mo binder phases. Ceram, *44*, 2283-2291.

© European Powder Metallurgy Association (EPMA)

[5] Correa, E.O.; Santos, J.N.; Klein, A.N. (2010). Microstructure and mechanical properties of WC Ni–Si based cemented carbides developed by powder metallurgy. Int J Refract Hard Met., *28*, 572-575.
[6] Li, H.; Yan, L.; Meng, L.; Li, Y.; Ai, F.; Zhang, H.; Jiang, Z. (2012). Effect of Ni on the Microstructure and Diffusion Behavior at the Interface of WC/High-Speed Steel Composites*.* Metals., *11*, 341.
[7] Rong, H.; Peng, Z.; Ren, X.; Peng, Y.; Wang, C.; Fu, Z.; Miao, H. (2012). Ultrafine WC–Ni cemented carbides fabricated by spark plasma sintering. Mater. Sci. Eng. A., *532*, 543-547.
[8] Human, A.M.; Northrop, I.T.; Luyckx, S.B.; James, M.N. (1991) A comparison between cemented carbides containing cobalt- and nickel-based binders. J Hard Mater., *2*, 245-256.
[9] Guilemany, J.; Sanchiz, I.; Mellor, B.; Llorca, N.; Miguel, J. (1993-1994). Mechanical-property relationships of Co/WC and Co Ni Fe/WC hard metal alloys. Int J Refract Metals Hard Mater. *12*, 199-206.
[10] Garcia, J.; Cipres, V. C.; Blomqvist, A.; Kaplan, B. (2019). Cemented carbide microstructures: a review., Int J Refract Hard Met., *80*, 40-68.
[11] Liu, X.; Song, X.; Wang, H.; Liu, X.;Tang, F.;Lu, H. (2018). Complexions in WC-Co cemented carbides. Acta Materialia.,*149*, 164-178.
[12] Peng, Y.; Buchegger, C.; Lengauer, W.; Du, Y.; Zhou, P. (2016). Solubilities of grain-growth inhibitors in WC-Co-based cemented carbides: Thermodynamic calculations compared to experimental data. Int J Refract Metals Hard Mater., *61*, 121-127.
[13] Li, G., Peng, Y., Yan, L., Xu, T., Long, J., & Luo, F. (2020). Effects of Cr concentration on the microstructure and properties of WC-Ni cemented carbides. J. Mater. Res. Technol., *9*, 902-907.
[14] Wittmann, B.; Schubert, W. D.; Lux, B. (2002). WC grain growth and grain growth inhibition in nickel and iron binder hardmetals. Int J Refract Hard Met., *20*, 51-60.
[15] Huang, S. G.; Liu, R. L.; Li, L.; Van der Biest, O.; Vleugels, J. (2008). NbC as grain growth inhibitor and carbide in WC–Co hardmetals. Int J Refract Hard Met., *26*, 389-395.
[16] Buchegger, C.; Lengauer, W.; Bernardi, J.; Gruber, J.; Ntaflos, T.; Kiraly, F.; Langlade, J. (2015). Diffusion parameters of grain-growth inhibitors in WC based hardmetals with Co, Fe/Ni and Fe/Co/Ni binder alloys. ., Int J Refract Hard Met., *49*, 67-74.
[17] Huang, S.; Liu, R.L.; Lib, L.;Van der Biest, O.; Vleugels, J. (2008). NbC as grain growth inhibitor and carbide in WC–Co hardmetals. Int J Refract Hard Met., *26*. 389-395.
[18] Acchar, W.; Revoredo de Macedo, H. (2005). Influence of NbC-Addition on Mechanical Properties of WC-Co. Materials Science Forum. (Vols. 498–499, pp. 363–368). Trans Tech Publications.
[19] Ismail, A.; Abd Aziz, N. (2014). Corrosion Behavior of WC-Co and WC-Ni in 3.5% NaCl at Increasing Temperature. In Applied Mechanics and Materials (Vol. 660, pp. 135–139). Trans Tech Publications
[20] Tarragó, J.M.; Ferrari, C.; Reig, B.; Coureaux, D.;Schneider, L.; Llanes. L. (2015) Mechanics and mechanisms of fatigue in a WC–Ni hardmetal and a comparative study with respect to WC–Co hardmetals, Int. J. Fatigue., *70*, 252-257.
[21] Phuong, D.D; Trinh, P.V.; Duong, L.V.; Chung L.D. (2016). Influence of sintering temperature on microstructure and mechanical properties of WC-8Ni cemented carbide produced by vacuum sintering, Ceram., *42*, 4937-14943.
[22] G. Petzow, Materialkundlich-technische Reihe, Vol. 1: Metallographisches, keramographisches, plastographisches Ätzen (Borntraeger, Berlin, Stuttgart, 1994) [ger].
[23] Pharr, George M.; Herbert, Erik G.; Gao, Yanfei (2010). The Indentation Size Effect: A Critical Examination of Experimental Observations and Mechanistic Interpretations. Annual Review of Materials Research, 40(1), 271–292. doi:10.1146/annurev-matsci-070909-104456

© European Powder Metallurgy Association (EPMA)